Phase Sensitivity Characterization in Fiber-optic Sensor Systems Using Amplifiers and TDM

Yi Liao, Ed Austin, Philip J. Nash, Stuart A. Kingsley, *Senior Member, IEEE*
and David J. Richardson, *Senior Member, IEEE* [1]

***Abstract*—We present an analytical approach to accurately model the phase sensitivity, and provide simple analytical formulae, useful in the design, comparison and optimization of multiplexed amplified interferometric fiber-optic based sensor systems. The phase sensitivity model incorporates the various key noise contributions including receiver noise, amplified spontaneous emission (ASE) induced noise, active sources noise and other phase noise terms. We define and present a novel term 'Demod phase sensitivity' to take into account the effects from noise aliasing in systems based on time division multiplexed (TDM) architectures. An experiment was conducted that confirmed the appropriateness and accuracy of the phase sensitivity model. The approach is widely applicable but particular appropriate for fiber-optic sensor systems using amplifiers and TDM.**

***Index Terms*—Phase noise model, phase sensitivity, interferometric fiber optic sensor, amplified array, TDM, noise aliasing, derivative approach**

I. INTRODUCTION

Interferometric fiber optic sensors have been researched for nearly four decades, the interest driven by a number of practical applications, particularly in military sonar and in seismic surveying [1]. Fiber sensors provide many advantages over conventional electro-ceramic-based sensors, including their immunity to electromagnetic interference, high sensitivity, simplicity, smaller cross-section, potential lower cost, multiplexing capability and especially their reliability in underwater applications.

Interferometric fiber optic acoustic sensors are based on measuring the phase change of light travelling in an optical fiber due to the strains developed on the fiber by an applied measurand. The non-linear response between the optical phase modulation and the intensity output of the interferometer is linearized by methods including both feedback and open-loop demodulators [2]. The performance of any demodulation scheme is always limited by various types of intensity or phase noise such as shot noise, thermal fluctuations, optical source noise, electronic drift and other system specific sources of noise [1]. Understanding the impact of these various forms of noise is important since they define the ultimate phase sensitivity of a sensor system. In general, the phase sensitivity, which determines the minimum phase change that can be detected, is the key fundamental performance metric used to characterize most interferometric sensing systems. If we know the noise sources in a sensor system, the system phase sensitivity can in principle be predicted. Usually the typical single-mode all-fiber interferometer is an intrinsically 'quiet' device, and the electro-optic system used to interrogate the sensor establishes the noise limitations.

However, even with the ultra-high phase sensitivity available, single channel applications are only appropriate in just a few instances for cost reasons. In most optical sensor systems, each laser is used to interrogate as many sensors as possible to amortize the cost of the laser over as many TDM channels as possible. While this reduces the overall cost of the system, it also introduces a common source of noise. For normal operation of a single sensor the phase noise typically exhibits a $1/\sqrt{f}$ low frequency component with a corner frequency ~100 kHz, and the high frequency white noise component is of no consequence. However, in systems based on time division multiplexing, at most detection frequencies, the high frequency phase noise components can be aliased to produce excess noise in the baseband spectrum which can limit the sensor sensitivity [3, 4]. Anti-aliasing filters cannot be used to eliminate the high frequency phase noise since it is an intrinsic noise component of the system. High frequency noise terms in the optical signal will alias in-band, and elevate the sensor noise floor. It can rapidly limit the phase sensitivity that can be achieved.

Many other multiplexing schemes have also been proposed and investigated in current fiber-optical sensor systems based on techniques including frequency, coherence, and wavelength multiplexing, and combinations thereof [5-9]. In each instance, splitting/recombination loss ultimately limits the scalability of the approach, with the number of fibers required for telemetry a further critical factor that significantly impacts the overall system cost and practicality. Fortunately, however, optical amplifiers can be incorporated into these systems to compensate the distribution loss and to decrease the insertion loss of the array [8, 10]. But amplifier placement in the system has a major impact on noise performance. They produce a background radiation known as amplified spontaneous emission (ASE), which is responsible for the noise of the

[1]Manuscript received September, 2012.

Yi Liao and David J. Richardson are with the Optoelectronics Research Centre, University of Southampton, UK (phone: 44-23-80595343. e-mail: yil@orc.soton.ac.uk, djr@orc.soton.ac.uk).

Ed Austin, Philip J. Nash and Stuart A. Kingsley are with TGS, Surrey KT6 6AP, UK (e-mail: Ed.Austin@tgs.com, Phil.Nash@tgs.com, skingsley@fiberdyneoptoelectronics.com).

device. At the detector, the ASE signal generates two new noise terms known as the signal–spontaneous and the spontaneous–spontaneous beat noise. They are the result of the broadband ASE signal mixing with both the signal and itself at the detector. Most fiber-optic sensor systems that make use of optical amplifiers incorporate several such devices, and the amplifier placement can have a significant impact on the overall phase sensitivity [5, 11]. This impact can be expressed by the dependence of the phase sensitivity on the optical signal to noise ratio (OSNR), which denotes the ratio of the optical signal power to the ASE noise power in sensor systems incorporating either lumped or distributed amplifiers.

However, there is no full phase sensitivity analysis which covers all the factors above. It is the purpose of this paper to develop a full and systematic phase noise model applicable to interferometric fiber optic systems. In this paper, we present a general phase noise analysis applicable to all interferometric fiber optic sensors, including systems based on amplification and TDM technology as applied to our specific optical architecture. The system noise analysis includes all the potential noise sources in general sensor systems, together with noise aliasing in TDM architectures. This phase sensitivity model provides a general analytical approach to evaluate, characterize, compare and optimize the performance of fiber sensor systems. We validate the model with a pulsed interferometric fiber-optic sensor system incorporating a novel derivative interrogation approach which has the benefit of mitigating the system noise and avoiding overscale problems (as discussed later in the paper).

In section II, we demonstrate the operational principle of a general pulsed interferometric fiber-optic sensor system. Section III then discusses the interrogation of phase changes in such a sensor and describes the various sources of system noise. In Section IV we analyze noise aliasing in TDM based systems. In Section V, we demonstrate an experimental pulsed interferometric TDM sensor system, based on a novel derivative based interrogation approach and discuss the measured system phase noise floor. Section VII discusses the sources of noise within the experiment and compares the measured phase noise floor with the predicted results. Finally, our conclusions are summarized in Section VII.

II. General Operation Principle

We start by considering the operational principle and phase sensitivity of pulsed interferometric sensor systems. For convenience we consider a Michelson interferometer with pulsed heterodyne detection as our exemplar system as it provides a practical approach to interferometric sensor systems. Our results however are general.

A typical configuration is illustrated in Fig. 1. The input light is pulsed, frequency-shifted and split into two fibers through a 50:50 fiber coupler, which can be thought of as generating a signal and a reference beam. The signal beam is exposed to the measurand, whereas the reference beam is usually shielded. The two beams are reflected back into the same coupler by Faraday mirrors (FRM) where they are combined and interfere. The resulting beam in the up-lead fiber is then fed into the demodulator system where the measurand induced phase modulation on the signal arm is detected and demodulated.

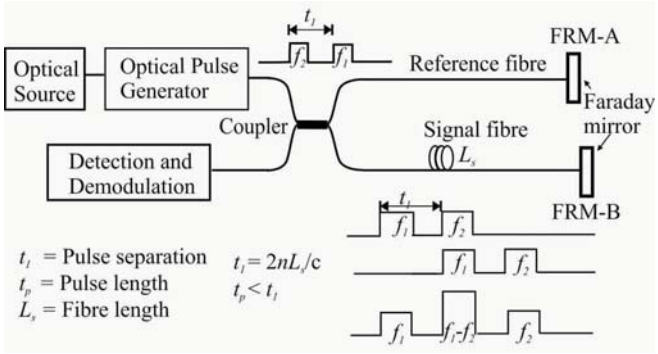

Fig. 1 Pulsed fiber-optic Michelson interferometric sensor system configuration with time domain diagram.

The timing diagram of the pulses in the system is also shown in Fig. 1. The interferometer sensor is interrogated with two optical pulses with frequencies of f_1 and f_2 separated in time by a period $t_1 = 2nL_s/c$ (which is twice the transit time in the sensor fiber of length L_s), and n is the effective refractive index of the fiber. The optical pulse pair is reflected from the two mirrors and is transmitted back to the interrogator unit. Because the optical pulse separation is arranged to be twice the transit time of light through the sensor, the reflection of the first optical pulse from FRM-B arrives at the receiver at the same time as the reflection of the second optical pulse from FRM-A.

The two reflections will therefore overlap at the receiver to produce a single pulse with a frequency equal to the frequency difference between the two pulses (at the carrier frequency $\omega_{IF} = 2\pi(f_1 - f_2)$), as shown in Fig. 1. This pulse carries all the phase change information from the signal arm imposed as a phase modulation of the carrier frequency (because the first pulse has been through the coil twice and has been exposed to the signal-induced phase change, whilst the second pulse has not). The output pulse train therefore comprises one sensor pulse at the carrier frequency carrying the measurand (as experienced in the signal arm), together with two "dead" pulses which correspond to the reflection of the first pulse from FRM-A and the reflection of the second pulse from FRM-B.

The optical pulse train (i.e., one sensor pulse plus two dead pulses) is received by a photodiode which converts the optical pulses into electrical pulses. The pulses are sampled by an analogue-to-digital converter (ADC) which then routes the digitized signals to the demodulator.

III. Noise in General Systems

The photodiode current for the received pulse from a general interferometric sensor system is represented by

$$i_{ph}(t) = P_s \mathrm{R}[1+\cos(\omega_{IF}t + \varphi_s(t))], \quad (1)$$

where

$R = e\eta/hv$ is the photodiode responsivity in A/W ,
P_s is the average receiver power,
ω_{IF} is the modulated intermediate frequency between optical angular frequencies of the two pulses,
$\varphi_s(t)$ is the phase modulation imposed on the heterodyne signals from the applied strain on the sensor fiber,

We now calculate the expected phase noise density in a general pulsed interferometric sensor system based on the following parameters:

1) Heterodyne signal power P_s,
2) Accumulated ASE noise spectral density S_{ASE} in one polarization mode per unit bandwidth,
3) Power spectral density of the frequency noise of the laser,
4) Power spectral density of the relative intensity noise of the laser,
5) RF generator noise,
6) Receiver noise.

The photodiode signal is DC filtered and sampled, and then routed to a particular phase demodulation system. All the sources of noise produced in the sensor system can be sorted to phase noise terms $n_\varphi(t)$ and intensity current noise terms $i_n(t)$, and the filtered received current with noise can be extended to

$$i_{ph}(t) = P_s R[\cos(\omega_{IF}t + \varphi_s(t) + n_\varphi(t))] + i_n(t), \quad (2)$$

The response between the optical phase modulation in the heterodyne signal and the intensity out of the interferometer is linearized by the demodulation operation, and the phase noise amplitude induced by the intensity noise is equal to the noise to carrier ratio [12]

$$\delta\varphi_{in} = \frac{\sqrt{\langle i_n^2(t)\rangle}}{RP_s}, \quad (3)$$

This is the relationship we will use later to interpret the conversion of intensity noise to system phase noise.

The intensity noise power at the receiver is fundamentally limited by the signal shot noise. However, in practice, receiver noise, ASE beat noise, AOM driver noise, and laser noise will be present and will dominate.

A. Receiver noise

We assume the signal power and ASE power to the receiver are P_s and $P_{ASE,}$ respectively .The photon shot noise generated at the receiver is given by

$$\overline{i_{sh}^2} = 2e\overline{i(t)}B = 2eR(P_s + P_{ASE})B, \quad (4)$$

where B is the detection bandwidth. $P_{ASE} = 2S_{ASE}B_O$ is the ASE noise spectral density in the bandwidth of the receiver optics B_O.

The receiver's electronic circuit also introduces some thermal noise at the receiver, which may limit the sensitivity of our sensor, and can be induced by a white current noise of $\overline{i_{receiver}^2}$.

B. Amplified spontaneous emission induced noise

In systems incorporating multiple amplifiers, the signal (S) to ASE beat noise, ASE to ASE beat noise and ASE shot noise at the receiver will contribute to the noise floor. The power spectral density of the signal to ASE beat noise, and the ASE-ASE beat noise are given by (5) and (6) at the receiver, respectively

$$\sigma_{S-ASE}^2(f) = 8R^2 P_S S_{ASE} \quad (5)$$

$$\sigma_{ASE-ASE}^2(f) = 4R^2 S_{ASE}^2 B_O (1 + \frac{f}{B_O})(1 + \frac{\cos 2\pi f t_1'}{2}). \quad (6)$$

C. Noise from active sources

Other noise sources that will degrade the phase sensitivity are: laser frequency noise, laser intensity noise and noise from the RF (radio frequency) oscillators employed to drive the optical pulse generator. Other noise sources are sufficiently small to be ignored. The frequency noise from the laser is converted to phase noise by the interferometer and is proportional to the path imbalance *d* in the interferometer, thus the phase noise spectrum density $\delta\varphi_{freq}(f)$, in rad/√Hz, due to the laser frequency noise spectrum density $\delta\nu(f)$ can be given by

$$\delta\varphi_{freq}(f) = \frac{2\pi nd}{c}\delta\nu(f) \quad (7)$$

The RF drive (used in practice to apply the frequency shift between the two interrogation pulses via an acousto-optic modulator (AOM)) introduces phase fluctuations. When the modulation sidebands are very small due to noise, i.e., if the phase deviation is much smaller than 1 rad, the spectral density of the phase fluctuation (phase noise) in rad^2/Hz is given by the approximation $S_{\Delta\varphi}(f) = 2\mathrm{L}(f)$, where $\mathrm{L}(f)$ is the single sideband noise (SSB) density. The spectral density of the resultant phase fluctuation from two similar oscillators is twice that associated with one oscillator, and is given by $S_{\Delta\varphi}(f)_{beat} = 2S_{\Delta\varphi}(f)$ .Thus the equivalent noise contribution due to the RF generator, in rad/√Hz, is given by,

$$\delta\varphi_{RF}(f) = \sqrt{4\mathrm{L}(f)} \quad (8)$$

Relative intensity noise (RIN) in dBc/Hz from the laser is equivalent to amplitude modulation of the optical signal, causing the RIN spectrum to appear as amplitude modulation sidebands around the carrier. The RIN will get reduced by 3 dB in an interferometer. We assume that the contribution to

the RIN due to the DC term in (1) is negligible when deriving our results. This is generally true particularly when the heterodyne carrier frequency is high. Thus, the equivalent noise contribution due to the RIN is,

$$\delta\varphi_{RIN}(f) = \sqrt{10\,\hat{}\,[(RIN(f)-3)/10]}. \quad (9)$$

D. Other phase noise sources

At the output of each amplifier, the ASE noise will not only add amplitude noise, but also adds phase noise to the amplified signal field [13]. Averaging over a large number of random phase variation events, we can obtain a standard phase deviation:

$$\delta\varphi_{ASE-PHASE} = \sqrt{\langle \delta\phi^2 \rangle} = \frac{1}{\sqrt{2}}\frac{E_{ASE}}{E_s}, \quad (10)$$

in which E_{ASE} is the ASE noise within the optical linewidth of the signal source, and E_s is the amplified signal power. This noise only applies a phase deviation to the phase signal, but the intensity dependence of the refractive index can lead to self-phase modulation (SPM) and cross-phase modulation (XPM) [13, 14], the variance of the phase fluctuations at the receiver produced by the amplitude fluctuations from the in-phase component, along the line, which is called Gordon-Mollenauer noise and is described by

$$\delta\varphi_{G-M} = 0.0054 L_{eff} S_{ASE}, \quad (11)$$

in which L_{eff} is the conventional effective nonlinear interaction length in km and the S_{ASE} in W. Note that the Gordon-Mollenauer noise is always referred to as a nonlinear phase shift. Compared with other noise sources, this noise source can be ignored when the transmission length is far less than 1 km.

The overall phase sensitivity of the sensor is given by the square root of the sum of the squares of each noise source discussed above, assuming the noise sources are statistically uncorrelated. Thus the total phase noise can be expressed as

$$\delta\varphi_{total} = \sqrt{\frac{\langle i_{sh}^2 \rangle + \langle i_{receiver}^2 \rangle + \sigma_{S-ASE}^2 + \sigma_{ASE-ASE}^2}{(P_S R)^2} + \delta^2\varphi_{freq} + \delta^2\varphi_{RIN} + \delta^2\varphi_{RF} + \delta^2\varphi_{ASE-PHASE} + \delta^2\varphi_{G-M}} \quad (12)$$

IV. Noise Aliasing in TDM

TDM is a typical multiplexing approach used for pulsed sensor systems. Sensors are sequentially addressed using the pulsed input signal such that the time of flight of optical pulses in the multiplexed array allows individual sensor signals to be distinguished.

Noise aliasing of high frequency components is one of the common issues associated with all TDM architectures [3, 4]. TDM architectures inherently sample each sensor at the interrogation repetition rate which depends on the number of TDM sensors, and the length of fiber per sensor, which determines the inherent bandwidth available for the phase modulated signal to occupy. With limited interrogation repetition rates in multiplexed systems, the high frequency phase noise components can be aliased to produce excess noise in the baseband spectrum which can limit the sensor sensitivity [3, 4]. Anti-aliasing filters cannot be used prior to digitization to eliminate the high frequency phase noise since it is an intrinsic noise of the system.

The effect of noise aliasing can be assessed by accumulating the noise contributions at frequencies centered at harmonics of F_s in their noise spectra. The aliased noises determine the system's final performance. To account for the noise aliasing effect in TDM architectures, we introduce the 'Demod phase sensitivity' to characterize the phase sensitivity after demodulation in a sensor system. For a given electrical detection bandwidth of B_e and a pulse repetition rate of F_s, the effect of noise aliasing at a signal frequency of f_m is given by

$$\delta\varphi_{\text{Demod}} = \mu\sqrt{\sum_k \left[2 \sum_{q=0}^{(B_e - f_e - f_m)/F_s} \delta\varphi_k^2(f_e + f_m + qF_s) \right]}. \quad (13)$$

in which μ represents a factor accounting for the subtraction operation in the demodulation, $\mu = 1$ for normal signals of which no subtraction process is involved in the demodulation, $\mu = \sqrt{2}$ for derivative signals (see Section V). k stands for the subscript of different noise sources, including shot, receiver, S-ASE, ASE-ASE, RIN, RF, and laser frequency noise. f_e denotes the effective starting frequency to be aliased for different noise sources, which depends on the particular demodulation approach used.

Most of the sources exhibit white noise properties and when the frequency noise from the laser and the RF generator are small [15], the 'Demod phase sensitivity' can be simplified to

$$\delta\varphi_{\text{Demod}} = \frac{2B_e\mu}{F_s}\sqrt{\sum_k \delta\varphi_k^2(f_m)}. \quad (14)$$

The term 'Demod phase sensitivity' provides an effective way to compare the performance of various interferometric fiber-optic based sensor systems, combining the noise contributions from both the array architecture and the interrogation technology employed.

V. Experimental Setup and Results

A. Experimental arrangement

To validate the developed phase noise model, we configured an experimental setup of a pulsed interferometric sensor system, as shown in Fig. 2. This sensor system comprises three principal components: a transmitter, a multiplexed sensor array and a receiver section.

The transmitter consists of four narrow linewidth (~10 kHz) fiber lasers (NP Photonics' Rock Single Frequency Narrow Linewidth Fiber Laser Module) as interrogation sources. These were multiplexed, pulsed, frequentcy-shifted, and

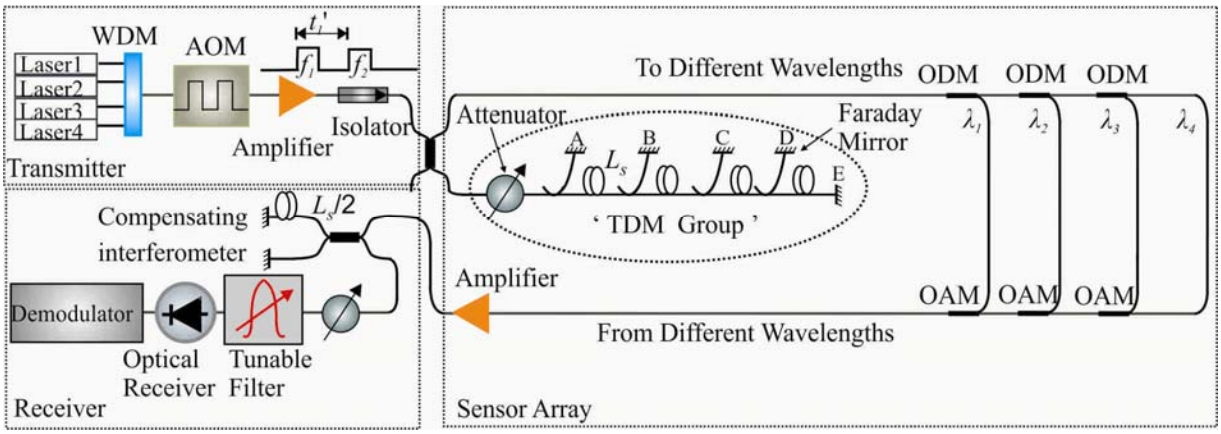

Fig. 2 Experimental setup for the time division multiplexed pulsed interferometric sensor system to validate the phase noise mode. WDM: Wavelength division multiplexer; AOM: Acoustic-Optic Modulator; ODM: Optical drop multiplexer; OAM: Optical add multiplexer. L_s: Length of the sensing fiber.

amplified, then launched into the sensor array. The maximum launch power into the array was +22 dBm per wavelength, limited by nonlinear effects.

The experimental arrangement was constructed with only one "TDM group" representing all the multiplexed sensors in an array. This was located before a four wavelength multiplexed network so that each wavelength suffered the loss of this device. This should provide similar optical performance in terms of loss to a fully loaded system in which a TDM group is included at each wavelength between each ODM/OAM pair and is obviously far more convenient from a practical perspective. The "TDM group" itself comprised a lab 4C sensor package along with a tunable attenuator to simulate a prescribed number of additional "missing sensors". The lab 4C sensor package is made of a cluster of three orthogonally mounted accelerometers and a hydrophone as described in [16]. Later we will show the measured phase noise floor of the sensors in the 4C sensor package for validation of the phase noise model.

The return signals from the array were mixed optically at a compensating interferometer, and attenuated before the demultiplexer to achieve a peak optical power of −20 dBm per wavelength at the receiver as required to obtain the desired shot noise limited performance. The demultiplexer was used to drop the signal bearing channels. The output of the demultiplexer was then detected and demodulated to extract the phase information.

B. Derivative approach

Some applications require very large dynamic range (i.e. >> ~120 dB) at low frequency. These generate signals that induce phase modulations that exceed the bandwidth of the interferometric phase measurement method. To overcome this, a technique is implemented that measures the rate of change of the phase, thus greatly reducing the bandwidth at low frequencies required for the induced phase modulation.

This operates by tracking the phase changes between successive optical samples [12]. We developed the TDM group (4C sensor package) based on an inline Michelson configuration, as illustrated in Fig. 2. In the operation, the pulse pair which is sent into the system is separated by a time delay equal to a single transit time of light through a sensor, i.e., $t_1' = nL_s/c$, and an additional optical compensating interferometer is added before the optical receiver. This circuit contains a delay coil which is equal to half a sensor coil in length. This means that the return transit time of light through this delay coil is equal to the optical pulse separation (t_1').

The system timing diagram is shown in Fig. 3. The two pulse trains returning from different reflectors in the sensor package no longer overlap because the pulse separation is only half the return transit time of light through a sensor coil. These two pulses trains have then each gone through the two paths within the compensating interferometer (one path involves going through the delay coil, and the other does not). There are two sets of pulse pair trains at the interferometer output, and because of the function of the delay coil, these sets now overlap with each other, as can be seen in Fig. 3 (c) and (d), to produce a single pulse with the carrier frequency ω_{IF}.

The timing is such that for, the reflection of the undelayed first pulse from the second reflector arrives back at the receiver at the same time as the reflection of the delayed second pulse from the first reflector. This is the normal sensor pulse. This pulse carries all the phase change from the first sensing fiber imposed as a phase modulation of the carrier frequency (because the first pulse has been through the coil twice and has been exposed to the signal-induced phase change, while the second pulse has not). The phase information from these pulses is the normal signal (from normal channels 2, 4, 6, 8 etc.).

It can also be seen from the pulse timing diagram that the undelayed reflection of the second pulse from the first reflector overlaps with the delayed reflection of the first pulse from the first reflector. Although these two pulses arrive back at the optical receiver simultaneously, and have been reflected

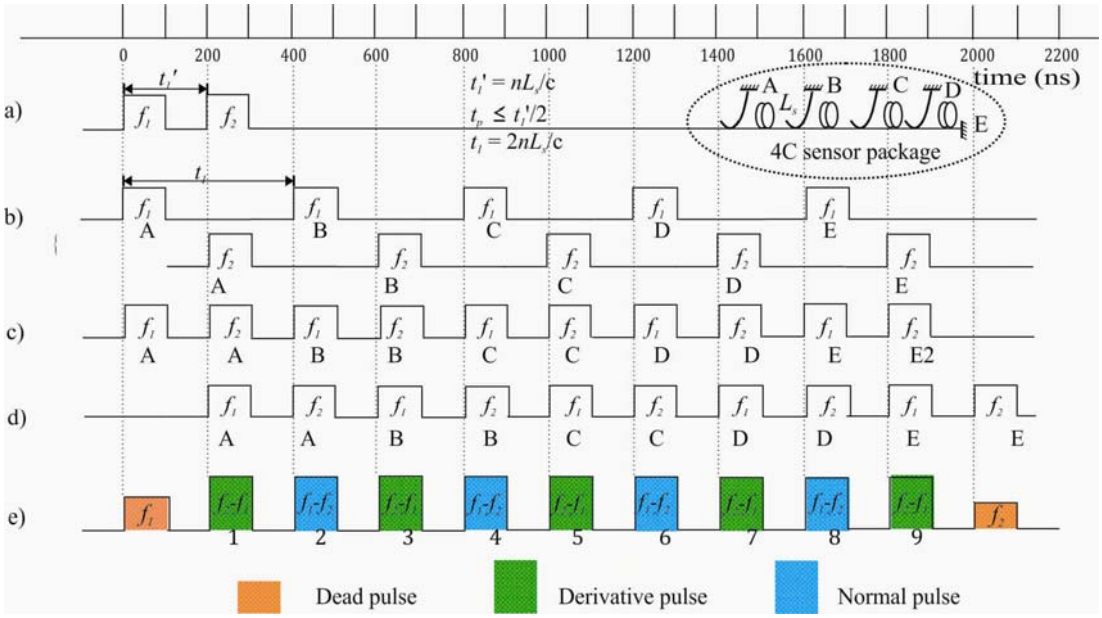

Fig. 3 System time domain diagram for the pulses (a) after the pulse generator, (b) reflected from the TDM group, (c) from the compensating interferometer without delay coil (d) from the compensating interferometer with delay coil (A: Delayed first pulse reflected from A, A:Delayed second pulse reflected from A, and so on), and (e) at the receiver. The output of the 4 sensors contains a pulse train of four sensor pulses, five derivative pulses, together with two "dead" pulses.

from the same point in the array, they were not reflected at the same time, but at a time interval equal to the pulse separation. They therefore carry a phase modulation which is directly proportional to the change of phase over this time interval. This phase modulation is therefore a representation of the differential of the phase at that point. We call this the derivative pulse.

The derivative pulses contain the derivative of the phase information at the points A, B, C, D and E in the array, and by subtracting the signals from point B from that for point A (channel 3 – channel 1), it is possible to obtain a signal which is a derivative of the signal from the first sensor. The signal from the second sensor is then obtained by subtracting the signal at Point C from that at point B (channel 5 – channel 3), and so on. The phase information demodulated from the subtraction of these derivative pulse pairs is the derivative signal (from subtracted derivative channels 3 − 1, 5 − 3, 7 − 5, etc.).

The derivative signals represent a measure of the rate of change of phase of each sensor. The amplitude of the phase change on each derivative sensor is frequency dependent, but at seismic frequencies (<175Hz) it is much lower than that of the "normal" sensor. At 800 Hz, the phase change on the derivative sensor is 60 dB lower than it is on the normal sensor and it decreases at 6 dB per octave, so that at 100 Hz it is 78 dB lower. The derivative signal can then be used in a number of different ways to reconstruct the normal signal even in overscale situations where the normal signal has exceeded the π/2 threshold between successive pulses. The derivative signal offer significant advantages in the seismic seabed industry since it provides a means to overcome or control signal oversizing (i.e. driving the sensor through multiple 2π phase shifts) which occurs frequently during the first break (i.e. the first direct water-borne arrival of the acoustic shots) when the acoustic energy is high.

Subtractions between different points within the system are used to obtain derivative signals, so that system noise components including optical power variations and vibrational pickup along the cable are mitigated. The derivative signals therefore give a much more 'lab friendly' method for measuring and comparing the system noise, because they are essentially insensitive to audio frequency acoustic pickup.

C. Experimental results

To validate the predicted phase noise and Demod phase sensitivity model above, the phase noise spectrum for one sensor in the 'TDM group' was tested. Fig. 4 shows the measured demodulated peak phase floor spectrum up to 5 kHz interrogated at 1545.32 nm with a TDM group insertion loss of 35 dB. The insertion loss of the 'TDM group' for the illustrated spectrum in the figure is close to the loss of a TDM group with 32 sensors addressed by a single wavelength according to current sensor technology [17]. The measured OSNR before the receiver from this loss was 30 dB.

The peak Demod phase noise floor for the normal signal (unreferenced) is found to be −74 dB re 1 rad/√Hz at 1.5 kHz. and is essentially flat from 200 Hz to 5 kHz. The higher noise in the spectrum at low frequency comes from environmental noise with the increasing background at low frequency due to laser frequency noise.

The system phase noise floor shows a flat spectrum for the derivative signal across the full frequency range. The measured value at 1.5 kHz is around −89 dB re 1 rad/√Hz, and the best achievable system sensitivity in the experimental

system is calibrated to be −91.5 dB re 1 rad/√Hz limited by the laser RIN, shot noise and receiver noise.

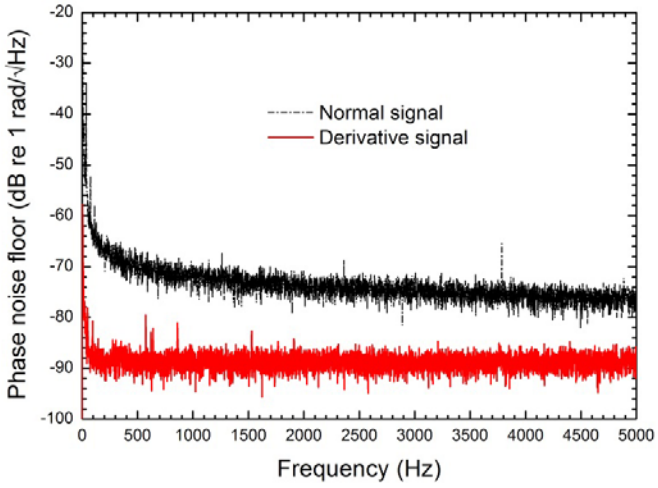

Fig. 4 Measured demodulated peak phase noise floor for the normal signal and the derivative signal from DC up to 5k Hz

VI. Discussion

Now that we have configured the experimental setup, we can calculate the Demod phase sensitivity from the characterization of the sources of noise in the setup.

A. Sources of noise in the system

The system's interferometric phase sensitivity is determined by a number of factors including the receiver noise, signal shot noise, amplifier noise, laser frequency noise and laser relative intensity noise as discussed in section III.

Fig. 5 demonstrates most of the measured and calculated noise sources in the experimental arrangement, from 10 Hz to 100 MHz, with a measured OSNR of 30 dB before the receiver. The OSNR is measured with a noise bandwidth of 0.1 nm. The measured OSNR is sufficient for us to predict the ASE noise spectral density S_{ASE}, which can be used in equation (5) and (6) to predict the ASE beat noise. The fitted laser frequency noise measured in an interferometer with a delay length of 40 m (the same as the sensor imbalance length) dominates all other noise sources, and ultimately limits the phase sensitivity in such systems. The measured laser RIN dominates the receiver noise, shot noise and ASE beat noise and is dominated by a peak at the relaxation frequency of the laser around 1 MHz but shot-noise limited otherwise. The RF oscillator noise has a 1/f spectrum. The contribution to the phase noise from an RF generator with a specified SSB of −120 dBc/Hz at 1 kHz offset is small. The contribution to the RIN due to the DC term in (1) is negligible since the heterodyne carrier frequency in the setup is 50 kHz. The ASE-ASE RIN exhibits an oscillating structure with a period determined by the delay length of the compensating interferometer. The ASE phase noise is sufficiently small to be ignored, as is the ASE-XPM noise, when the transmission distance is less than 1 km.

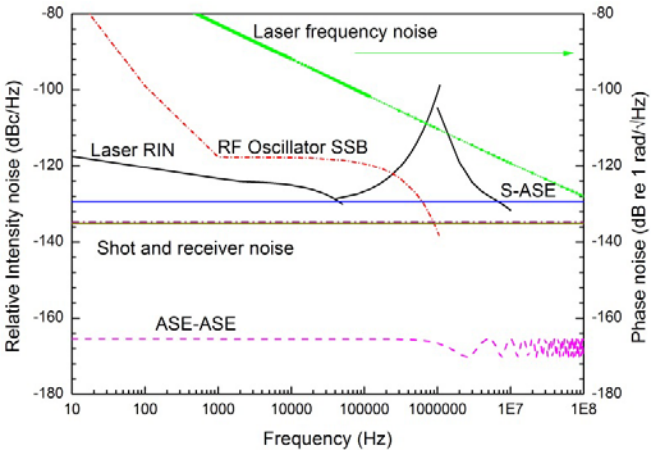

Fig. 5 Fitted noise spectra from measurements and prediction

B. Advantage of the derivative approach

The Demod phase sensitivity for the normal signal and the derivative signal can be derived from equation (13), which also indicates the advantage of the derivative signals over the normal signals.

In equation (13), the noise aliasing from the various noise sources that needs to be incorporated to calculate the Demod phase sensitivity varies according to the detailed noise spectra which are determined by detailed numerical calculations of the accumulated noise for each sampling period within their effective electrical bandwidths, supplemented with detailed measurements that allowed us to determine the noise properties of these individual sources, as illustrated in Fig. 5.

There are two differences in which the Demod phase sensitivity for the normal signal and derivative signal are calculated from equation (13). Firstly, the subtraction process used to get the derivative signal introduces $\mu = \sqrt{2}$, which doubles the total noise. However, although the derivative approach doubles the white noise sources it also eliminates the 1/f noise sources. The laser frequency noise in the Rock laser is dominated by 1/f noise components up to frequencies >10 MHz while the measured phase noise at high frequency is usually dominated by laser RIN. Thus, the subtraction process significantly reduces the dominant laser frequency noise induced phase noise by increasing the starting frequency f_e from DC to >10 MHz for the laser frequency noise source in equation (13), such that most of the aliasing noise components from the laser frequency noise are eliminated as shown in Table 1. In contrast for normal signals all the noise components across the entire electrical bandwidth down to DC contribute to the aliasing at the signal frequency f_m.

Table 1 summarizes the noise contributions at 1.5 kHz for all the sources of noise, and the Demod phase sensitivity for the normal signal and the derivative signal, respectively. It can be seen from the second column of the table that the frequency noise from the fiber laser dominates and introduces a total phase noise peak value of 95 μrad/√Hz at 1.5 kHz.

TABLE 1 NOISE SOURCES AND DEMOD PHASE SENSITIVITY AT 1.5 KHZ

Noise terms	*Phase noise (μrad/√Hz)*	*Demod phase sensitivity (μrad/√Hz)*	
		Normal signal	Derivative signal
Shot noise	0.18	6.4	9
S-ASE	0.25	8.7	12.3
ASE-ASE	0.0025	0.08	0.34
Receiver	0.15	5.2	7.33
Laser Freq.	**95**	**137.8**	**0**
Laser RIN	0.355	11.04	15.8
RF SSB	2	3.7	0
ASE-PHASE	0	0	0
G-M	0	0	0
Total peak value		−**74.1** dB re 1 rad/√Hz	−**89.7** dB re 1 rad/√Hz

It is can be seen from Table 1 that the Demod phase noise floor for the normal signal is still dominated by the aliased laser frequency noise, which is mitigated in the derivative signal. The contribution from the laser frequency noise increases to 137.8 μrad/√Hz due to the noise aliasing and remains the dominant noise for normal signals. However, it has been effectively reduced to zero for derivative signals, providing a Demod phase sensitivity value of −89.7 dB re 1 rad/√Hz, limited by the laser RIN, shot noise and ASE beat noise at the receiver. These values are given assuming a system averaged OSNR of 30 dB and for a received peak optical signal power of −20 dBm. The predicted Demod phase noise floor is very close to our measured phase sensitivity of −74 (normal) and −89 (derivative) dB re 1 rad/√Hz, respectively. Thus, the derivative approach shows significant improvement in the Demod phase sensitivity and provides an ideal lab tool to assess the system noise floor.

C. *Affects from ASE noise*

In systems incorporating amplifiers, the Demod phase sensitivity is limited by the ASE beat noise, which can be illustrated by the dependence of the phase sensitivity on the system OSNR. To characterize the phase sensitivity of the sensor system and investigate the model's dependence on the ASE noise, the system Demod phase sensitivity was averaged over the frequency range of 300 Hz to ~800 Hz for the derivative signal and 2 ~4 kHz for the normal signal, since it is deteriorated by environmental noise at low frequency. The characterized values as a function of the measured OSNR of the signal into the receiver are shown in Fig. 6. The various OSNR values were achieved by changing the insertion loss of the 'TDM group' in the setup. The points show the average value of the measured results and the curve indicates the calculated results from equation (13) for comparison. The measured values are in good agreement with the theoretical prediction.

It can be seen from the figure that the phase sensitivity in the normal channel is dominated by the laser frequency noise, thus, it remains independent of the OSNR when the average OSNR is larger than 15 dB (as is often the case).

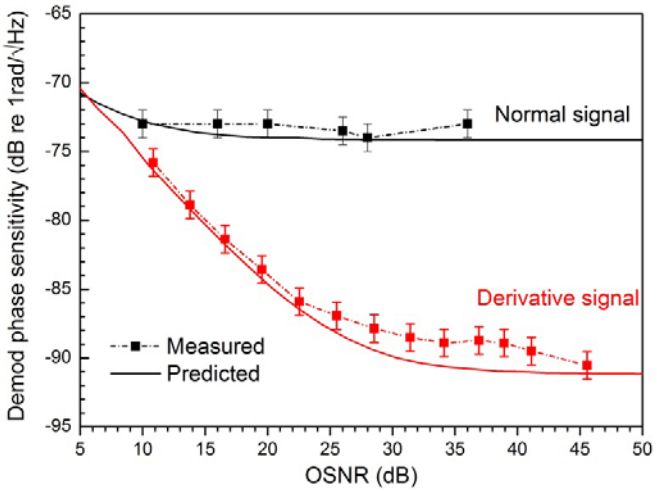

Fig. 6 Measured and predicted Demod peak phase sensitivity as a function of the measured average OSNR with an OSA before the receiver in the experimental arrangement

For the derivative signal, when the OSNR is better than 32 dB, the ASE beat noise can be ignored compared to the laser RIN. A system noise floor of −91 dB re 1 rad/√Hz was measured. The system noise floor is dominated by laser RIN and shot noise and thus is very sensitive to the injected optical power level at the receiver, so the measured value ranges from −88 to −91 dB re 1 rad/√Hz, which is 1 ~3 dB higher than the predicted ideal phase noise floor.

However, the phase sensitivity in an amplified multiplexed sensor system deteriorates with decreasing OSNR and will ultimately be dominated by ASE beat noise. When the OSNR is less than ~ 32 dB, the S-ASE noise starts to dominate, and the phase sensitivity deteriorates with a further decrease in the OSNR. The Demod phase sensitivity in large-scale amplified hybrid multiplexed sensor systems can be found in another paper [17].

VII. CONCLUSIONS

In conclusion, we have developed an analytical method to accurately predict the phase sensitivity of interferometric fiber-optic based sensor systems. The model covers all the potential phase noise sources and requires knowledge of the OSNR, laser frequency noise, laser intensity noise, intrinsic current noise in the receiver and RF generator noise. This model also introduces the term 'Demod phase sensitivity' to quantify the effect of noise aliasing from high frequency phase noise components. The aliasing effect is found to be determined by the interrogation repetition rate and depends on the interrogation technology employed and it varies according to the noise source spectra. The model is general and can be applied to any amplified fiber sensor systems with TDM architectures. The measured Demod phase sensitivity from the experimental arrangement of a sensor system using a derivative approach to remove the system phase noise and to increase the dynamic range validates our phase noise model. The most interesting result of our modeling is that the best Demod phase sensitivity of −91.5 dB re 1 rad/√Hz in the

experimental system is limited by the laser RIN, shot noise and receiver noise when the signal OSNR is better than 32 dB, and it deteriorates with an increase in ASE noise. To the best of our knowledge, this is the first report of a full analytical description of the phase sensitivity in interferometric sensor systems, combining both the effects from all the potential noise sources and the effect of the high frequency phase noise aliasing.

REFERENCES

[1] P. J. Nash, G. A. Cranch, and D. J. Hill, "Large scale multiplexed fibre-optic arrays for geophysical applications," *Industrial Sensing Systems,* vol. 4202, pp. 55-65, 2000.

[2] J. H. Cole, C. Kirkendall, A. Dandridge, G. Cogdell, and T. Giallorenzi, "Twenty-five years of interferometric fiber optic acoustic sensors at the Naval Research Laboratory," in *Washington Academy of Sciences*, 2004, pp. 40-57.

[3] T. A. Berkoff, A. D. Kersey, and A. Dandridge, "Noise aliasing in interferometric sensors utilizing phase-generated carrier demodulation," *Fiber Optic and Laser Sensors Vii,* vol. 1169, pp. 80-88, 1990.

[4] C. K. Kirkendal, A. D. Kersey, A. Dandridge, M. J. Marrone, and A. R. Davis, "Sensitivity limitations due to aliased high frequency phase noise in high channel-count TDM interferometric arrays," in *11th International Conference on Optical Fiber Sensors*, 1996, p. Fr14.

[5] C. K. Kirkendall and A. Dandridge, "Overview of high performance fibre-optic sensing," *Journal of Physics D: Applied Physics,* vol. 37, p. R197, 2004.

[6] G. A. Cranch and P. J. Nash, "Large-scale multiplexing of interferometric fiber-optic sensors using TDM and DWDM," *Journal of Lightwave Technology,* vol. 19, pp. 687-699, 2001.

[7] G. A. Cranch and P. J. Nash, "High multiplexing gain using TDM and WDM in interferometric sensor arrays," *Fiber Optic Sensor Technology and Applications,* vol. 3860, pp. 531-537, 1999.

[8] C. W. Hodgson, M. J. Digonnet, and H. J. Shaw, "Large-scale interferometric fiber sensor arrays with multiple optical amplifiers," *Opt Lett,* vol. 22, pp. 1651-3, Nov 1 1997.

[9] C. W. Hodgson, J. L. Wagener, M. J. F. Digonnet, and H. J. Shaw, "Optimization of large-scale fiber sensor arrays incorporating multiple optical amplifiers.," *Journal of Lightwave Technology,* vol. 16, pp. 218-231, 1998.

[10] G. A. Cranch, P. J. Nash, and C. K. Kirkendall, "Large-scale remotely interrogated arrays of fiber-optic interferometric sensors for underwater acoustic applications," *Ieee Sensors Journal,* vol. 3, pp. 19-30, Feb 2003.

[11] G. A. Cranch and P. J. Nash, "Large-scale arrays of interferometric fibre-optic sensors for applications in military surveillance and seismic surveying," in *14th International Conference on Optical Fiber Sensors*, 2000, pp. 260-263.

[12] T. A. Berkoff and A. D. Kersey, "Signal-processing techniques for absolute displacement strain sensing using a fiber interferometer," *Optics and Lasers in Engineering,* vol. 16, pp. 153-161, 1992.

[13] E. Desurvire, *Erbium-doped fiber amplifiers: principles and applications*: Wiley, 2004.

[14] J.P.Gordon and L.F.Mollenauer., "Phase noise in photonic communication systems using linear amplifiers," *Optical Letters,* vol. 15, p. 1351, 1990.

[15] D. Hill and P. Nash, "Fibre-Optic Hydrophone Array for Acoustic Surveillance in the Littoral," presented at the *Photonics for Port and Harber and Security*, 2005.

[16] P. J. Nash and A. Strudley, "High efficiency TDM/WDM architectures for seismic reservior monitoring," in *20th International Conference on Optical Fiber Sensors*, 2009, pp. T1-T4.

[17] Y. Liao, E. Austin, P. J. Nash, S. A. Kingsley, and D. J. Richardson, "Highly Scalable Amplified Hybrid TDM/DWDM Array Architecture for Interferometric Fiber-Optic Sensor Systems," *Journal of Lightwave Technology,* vol. 31, pp. 882-888, 2013.